Induction of Cancerous Stem Cells during Embryonic Stem Cell Differentiation*�S

Hiroaki Fujimori[‡§], Mima Shikanai[§], Hirobumi Teraoka[§], Mitsuko Masutani[‡], and Ken-ichi Yoshioka[‡§1]

From the [‡]Division of Genome Stability Research, National Cancer Center Research Institute, 5-1-1 Tsukiji, Chuo-ku, Tokyo 104-0045, Japan and the [§]Department of Pathological Biochemistry, Medical Research Institute, Tokyo Medical and Dental University, 2-3-10 Kandasurugadai, Chiyoda-ku, Tokyo 101-0062, Japan

Background: Cancer stem cells are responsible for tumorigenesis; however, the developmental process is poorly understood.
Results: Differentiating stem cells in aberrant environments are subjected to carcinogenic stress, leading to genomic instabilization, mutation inductions, and cellular transformation with stemness characteristics.
Conclusion: Aberrant environment for differentiation risks cancerous stem cell development.
Significance: This is the first report showing normal stem cell transformation into malignant counterparts and their process.

Stem cell maintenance depends on their surrounding microenvironment, and aberrancies in the environment have been associated with tumorigenesis. However, it remains to be elucidated whether an environmental aberrancy can act as a carcinogenic stress for cellular transformation of differentiating stem cells into cancer stem cells. Here, utilizing mouse embryonic stem cells as a model, it was illustrated that environmental aberrancy during differentiation leads to the emergence of pluripotent cells showing cancerous characteristics. Analogous to precancerous stages, DNA lesions were spontaneously accumulated during embryonic stem cell differentiation under aberrational environments, which activates barrier responses such as senescence and apoptosis. However, overwhelming such barrier responses, piled-up spheres were subsequently induced from the previously senescent cells. The sphere cells exhibit aneuploidy and dysfunction of the *Arf-p53* module as well as enhanced tumorigenicity and a strong self-renewal capacity, suggesting development of cancerous stem cells. Our current study suggests that stem cells differentiating in an aberrational environment are at risk of cellular transformation into malignant counterparts.

A tumor consists of a heterogeneous cell mass in which only a small portion of the malignant cells, *i.e.* cancer stem cells (CSCs),[2] are responsible for tumor initiation and propagation (1). In fact, CSCs identified in a variety of tumors demonstrate a capacity for self-renewal and differentiation, which is shared by normal stem cells (2). Although cancer stem-like cells can be induced from stem/progenitor as well as differentiated cells by oncogene overexpression (3, 4), it remains unclear how CSCs spontaneously develop.

In the initial stages of carcinogenesis cells accumulate DNA replication stress-associated lesions that are induced by aberrant growth acceleration or oncogene activation, resulting in the activation of barrier reactions for carcinogenesis such as cell cycle arrest, senescence, and apoptosis (5, 6). These cellular responses illustrate the competing forces of cancer progression and prevention. Genomic instability is invariably accompanied with these stages of cancer development (6, 7). Analogously, mouse embryonic fibroblasts (MEFs) can escape senescence and exhibit immortality through accumulation of DNA replication stress-associated lesions under continuous growth acceleration, which accompanies genomic instability (8) and *Arf/p53* mutations (9). However, unlike CSCs, immortalized MEFs show neither tumorigenicity nor stemness characteristics (10).

The difference between immortal MEFs and CSCs underlies the properties of stemness characteristics. In addition to the expression of undifferentiated marker genes, both somatic stem cells and CSCs show sphere-formation abilities and heightened expression of the ATP binding cassette transporter and glycolysis dependence (11, 12). Importantly, whereas these properties are widely observed in stem cells, including embryonic stem cells (ESCs) (13–16), immortal MEFs do not acquire such properties during immortalization. Unlike immortal MEFs, CSCs share specific profiles of cell-surface antigens with somatic stem cells (11). However, like immortal MEFs, CSCs also show genomic instability and mutations, which are unshared characteristics with normal stem cells (17).

The existing body of literature on stem cells suggests that carcinogenesis can be initiated in somatic stem cells when the cells are subjected to the same conditions of stress that induce MEF immortalization. However, this challenges the idea of stem cell homeostasis, which is strongly protected by niche environments from the induction of genomic instability and

transformation (18). In agreement with this argument, stem cells injected into heterotropic sites are strongly implicated in tumorigenesis, in association with environmental aberrancies for stem cell maintenance (19). Further supporting the notion of stem cell tumorigenicity in aberrant environments, embryonal carcinomas were developed from xenografts of inner cell masses from mouse blastocyst and derailed primordial germ cells from the migration track (20, 21). Moreover, a recent study suggested that oncogenesis could be triggered by a niche disruption, resulting in disordered differentiation (22).

Taken together with a report showing stem cell niche dysfunction as a result of aging (23), these studies motivated the hypothesis that differentiating stem cells can become CSCs upon exposure to carcinogenic stress in a process analogous to MEF immortalization.

MATERIALS AND METHODS

Cell Culture—Culture of mouse ESCs and embryoid body (EB) formation assays were performed as previously described (24). For differentiation, cloned ESCs maintained with Knock-Out Serum Replacement (Invitrogen) and ESGRO (mouse leukemia inhibitory factor (LIF); Millipore, Billerica, MA) were cultured in three kinds of medium consisting of Iscove's modified Dulbecco's medium (Invitrogen) supplemented with FBS (Invitrogen), newborn bovine serum (NBS; Sigma), or adult bovine serum (ABS; Invitrogen) at 20%. The piled-up spheres were stained by crystal violet (Sigma), and the number of spheres was counted. Populations at P6 + 14 days were harvested by employing 0.25% trypsin-EDTA (Invitrogen) and then cultured in each medium for further experiments. All the following experiments were performed using bulk populations without cloning. Primary MEF immortalization assays were performed as previously described (8). For detection of the phenotype with an abnormal p53 pathway, each population was cultured in medium containing hydroxyurea (HU) as previously described (25). Sphere formation assay was performed as previously described (26) with a little modification. Briefly, CD133-positive and -negative populations were seeded to NBS-med containing methylcellulose 4000 (Wako, Tokyo, Japan) for 4 days. For detection, spheres were attached to culture dishes and were stained by crystal violet after 2 days of attachment (Sigma).

β-Galactosidase Activity Detection—β-Galactosidase activity was detected as previously described (27). Briefly, cultured cells were fixed with 4% formaldehyde and then incubated in staining buffer (1 mg/ml 5-bromo-4-chloro-3-indolyl-β-D-galactopyranoside (X-gal), 5 mM $K_3Fe(CN)_6$, 5 mM $K_4Fe(CN)_6$, and 2 mM $MgCl_2$ in PBS).

Reverse Transcription-Polymerase Chain Reaction—RT-PCR and quantified RT-PCR were performed as described (24). Briefly, total RNA was extracted from cultured cells with an RNeasy kit (Qiagen, Tokyo, Japan) and treated with DNase I (Promega, Tokyo, Japan). cDNAs were synthesized from 1 μg of total RNA using Super Script III first-strand synthesis system (Invitrogen). Ampli Taq Gold PCR Master Mix (Invitrogen) or Power SYBR Green PCR Master Mix (Invitrogen) was employed for PCR reaction. The primer list is described in supplemental Table 1.

Antibodies, Immunostaining and Western Blotting—The antibodies used are listed in supplemental Table 2. Immunostaining and Western blot analysis were performed as previously described (8). Briefly, for Western blotting, proteins were transferred onto a nitrocellulose membrane and probed with appropriate primary antibodies. The membrane was incubated with corresponding secondary antibodies conjugated with horseradish peroxidase, and the antigen-antibody complex was visualized by Immobilon Western (Millipore). For immunostaining, cells were fixed with formalin and then treated with Triton X-100. After blocking with serum, they were incubated with each primary antibody and then detected with fluorescent secondary antibodies.

Chromosomal Instability Detection—Giemsa staining and flow cytometric analysis were performed as previously described (8). Briefly, mitotic cells prepared by nocodazole treatment were hypotonically swollen with 75 mM KCl and then fixed with Carnoy's solution (75% methanol, 25% acetic acid). They were stained with 4% Giemsa (Merck) solution.

Apoptosis Detection Assay—Terminal deoxynucleotidyl-transferase-mediated dUTP-biotin nick-end labeling (TUNEL) was performed with the *in situ* Apoptosis Detection kit (Takara Bio, Otsu, Japan). The TUNEL-positive cells were detected by FACSCalibur HG (BD Biosciences). The sub-G_1 population was quantified as previously described (28).

Detection of p53 Mutation—The p53 transcripts from each population were amplified from the cDNA from each population and cloned using the pGEM-Easy vector system (Promega), and then the clones were sequenced by an ABI PRISM 3700 DNA analyzer (Invitrogen).

Tumor Formation Assay—For the tumor formation assay, 10^6 cells suspended in 100 μl of serum-free medium were mixed with an equal-volume of growth factor-reduced Matrigel (BD Biosciences) and injected subcutaneously into NOD. CB17-Prkdc^{scid}/J (NOD-SCID) mice. Tumor weight was measured 4 weeks after injection. Tumors were dissolved by dispase (Invitrogen) in part, and total RNA was extracted.

Isolation of CD133-positive Cells—CD133 positive fractions of induced immortal-like cells (iICs) in NBS-med were isolated by a magnetic bead cell sorting or fluorescence activated cell sorting (FACS) technique as previously described (24, 29). Briefly, for magnetic bead cell sorting, Dynabeads (Invitrogen) were coated with CD133 antibody (eBioscience). The beads/antibody complexes were incubated with cells, then the CD133-positive fraction was collected by a magnetic particle concentrator (Invitrogen). RNA was extracted from CD133-positive and -negative populations and subjected to RT-PCR. For FACS, cells incubated with CD133 antibody conjugated with Alexa Fluor 488 were sorted by FACS Aria II system (BD Biosciences). CD133-positive and negative fractions were subjected to sphere formation assay. Details of employed antibodies are described in supplemental Table 2.

Chemical Treatment of Differentiating Cells—The differentiating cells 1 day after passage 3 in ABS medium were treated with 25, 75, or 200 ng/ml neocarzinostatin (NCS). After 1 day, cells were passaged with NCS(+) medium. After 3 days, medium was changed to NCS(−) medium. This procedure is illustrated in Fig. 4*E*.

For Akt or PARP inhibition, differentiating cells on P2 or P1 cells in NBS-med were subjected to 0.25 μM Akt inhibitor IV (Merck) for 4 days or 0.5 μM AZD2281 (Selleck Chemicals, Houston, TX) for 6 days, respectively. These procedures are illustrated in Fig. 8*A*. Cell numbers and the ratio of live/dead cells were calculated by a TC10 automatic cell counter (Bio-Rad).

Statistical Analysis—All statistical analyses were performed using at least three independent measurements. All error bars represent S.D. ($n - 1$). Analysis of variance followed by Bonferroni multiple comparison test (see Figs. 1*F* and 6*A*) or *t* test with Welch correction (see Figs. 2*G*, 4*D*, 6*C*, 6D*c*, 6*F*, 6*G*, and 7*B* and supplemental Figs. S4*D* and S5) was performed for assessment. *p* values <0.05 were considered to be significant. The *green asterisks* on Fig. 6*C* and 6*Dc* and supplemental Figs. S4*D* and S5 indicate significant differences in value between each sample and ESCs.

RESULTS

ESCs Differentiating in an Aberrant Environment Senesce After Serial Proliferation, Leading to the Development of Immortalized Sphere Colonies—To directly address whether differentiating stem cells in aberrant environments are subjected to stress for cellular transformation, the effects of changes in the differentiation culture conditions of ESCs were first assessed. Although ESC injection under a homotopic implantation into blastocysts shows normal embryogenesis, that under heterotopic transplantations leads to tumor development (teratomas or teratocarcinomas) (20). Based on this, we attempted to construct an *in vitro* model in which ESCs maintained with KSR/LIF medium were subjected to differentiation in the medium containing FBS-med, NBS-med, or ABS-med (Fig. 1*A*). Differentiating cells were passaged under unique ESC passage conditions to produce consistent cellular environments. As shown in Fig. 1*B*, ESCs differentiating under each condition initially grew but then stopped proliferation, showing altered morphologies while differentiating (Fig. 1*B*, *P3* and *P5 cells*, *arrows*). Cells in NBS-med typically become senescent, as demonstrated by their flattened and enlarged morphology and senescence-associated β-galactosidase activity (Fig. 1*C*). Such senescent cells were first observed at P3 and became dominant in the culture at P5 (Fig. 1*B*, *P3* and *P5*, *arrows*).

Surprisingly, analogous to MEF immortalization, continuous cultivation in NBS-med led to the emergence of re-proliferating colonies in the previously senescent cells (Fig. 1, *B* (see *panels NBS* at *P6 + 14 days*) and *D*). Because these proliferating cells were able to continuously proliferate more than 40 passages in an immortal manner (data not shown), we named them "induced immortal-like cells" (iICs). Intriguingly, iICs appeared with piled-up sphere morphology in LIF-free medium containing NBS (Fig. 1*D*). Whereas cultivation in FBS-med conditions also, subsequently, led to a small subset of continuously growing cells (cGCs) without showing a canonical senescent stage, piled-up colonies were rarely observed in FBS-med and ABS-med (Fig. 1*B*; *P6 + 14 days*, *E*, and *F*), suggesting that piled-up sphere development through senescence is dependent on differentiation culture

conditions. Similar to MEF immortalization (Fig. 1*G*), differentiating ESCs in NBS-med first senesced and then spontaneously developed re-proliferating cells. However, unlike immortalized MEFs, ESCs in NBS-med subsequently formed piled-up spheres that are characteristic of stem cells, suggesting that the induced colonies, in fact, are cancerous transformants possessing stemness characteristics.
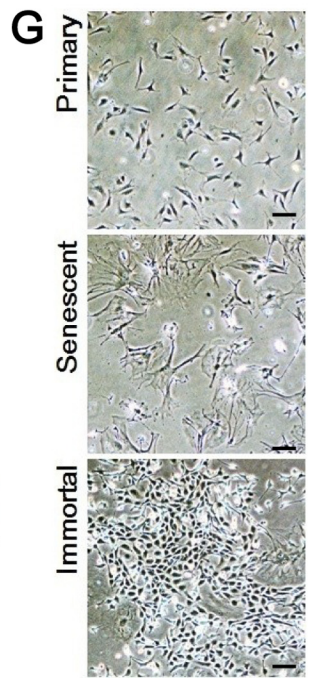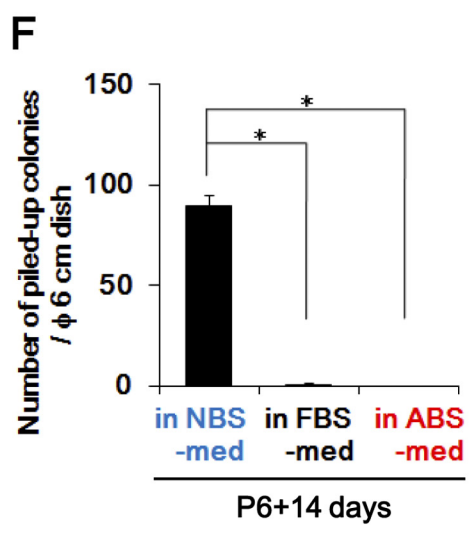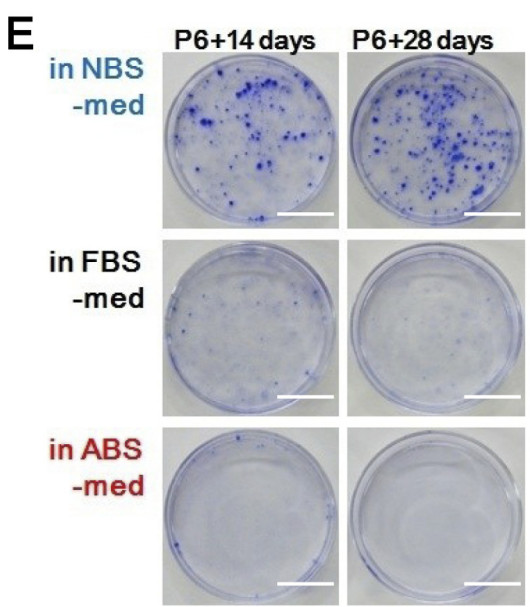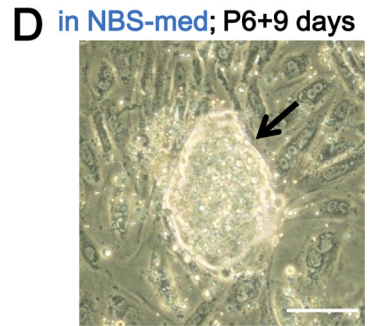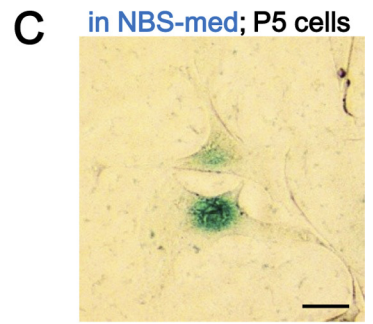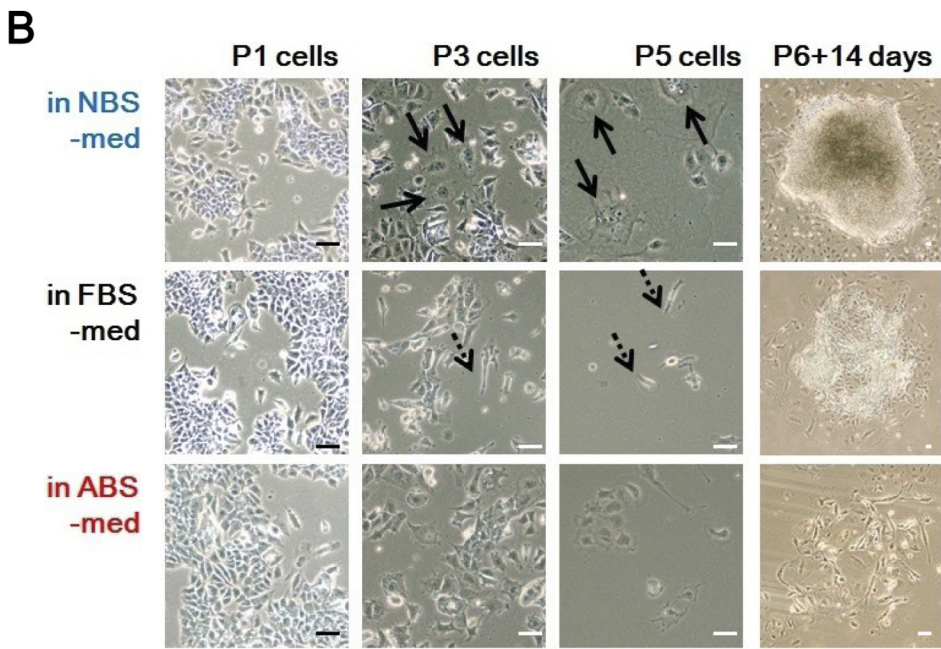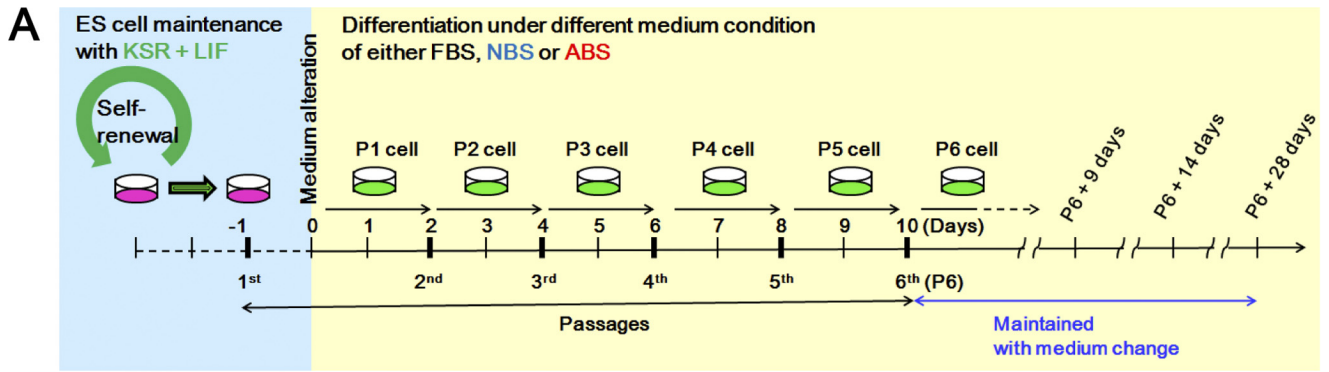
iICs in NBS-med Show Cancerous Characteristics—To determine whether the iICs, appearing in aggregates of sphere colonies, exhibited cancerous features, the cells were first assessed for genomic instability, which is a characteristic of cancer cells (30). As expected, the iICs showed aneuploidy, most of which is a common type of genomic instability in cancer cells, at P6 + 14 days in Giemsa staining of spread chromosomes (Fig. 2*A*) and in DNA content analysis using flow cytometry (Fig. 2*B*). Thus, the development of genomic instability accompanies immortal sphere formation in ESC-derived differentiating cells in NBS-med in a process analogous to carcinogenesis.

Because most cancer cells are mutated in either *Arf* or *p53* in a mutually exclusive manner and lose the function of Arf-dependent p53 activation (31), the mutation status of *p53* in the iICs in NBS-med was determined. In contrast to the original ESCs, *p53* mutations were observed in the iICs in as many as 7 of 10 transcripts, including six independent mutations (Fig. 2*C*). Next, to determine the status of functional loss of the *Arf/p53* pathway, p53-mediated senescence-like arrest was investigated using treatment with a low dose of HU, which induces DNA replication stress but allows continuous proliferation in *p53*-mutated populations (25). Although the cGCs in FBS-med as well as primary MEFs were completely arrested by HU treatment (supplemental Fig. S1*C*), the iICs in NBS-med still proliferated under HU treatment conditions (Fig. 2, *D* and *E*), suggesting p53 dysfunction. Taken together, our results demonstrated that iICs in NBS-med show genomic instability and functional loss of the p53 pathway. However, such properties of genomic instability and p53 dysfunction have been observed even in non-tumorigenic immortal MEFs (9), posing a question on the tumorigenicity of cancerous characteristics.

When iICs in NBS-med were injected into NOD-SCID mice, the resulting tumors were significantly larger compared with the original ESCs (Fig. 2*F*), indicating increased tumorigenicity of the iICs in NBS-med. Thus, our results together suggested that the iICs in NBS-med were indeed cancerous cells. Whereas genomic instability and mutations in the *Arf/p53* module were also observed in immortalized MEFs, further tumorigenicity is a feature unique to CSCs. Therefore, unlike immortal MEFs, the iICs in NBS-med derived from ESCs might accompany the acquisition of stemness characteristics.

iICs in NBS-med Show Properties of Stem Cells—Stem cell properties are represented by the expression of stemness marker genes and the capacity for self-renewal and differentiation, which are shared by somatic stem cells, ESCs and CSCs (2). The iICs in NBS-med showed strong expression of the pluripotent marker genes (*Klf4*, *Nanog*, and *Oct3/4*) and of the differentiation marker gene *CD133* along with weak expression of *Cdx2* and *T* (Fig. 3*A*), indicating that the iICs in NBS-med
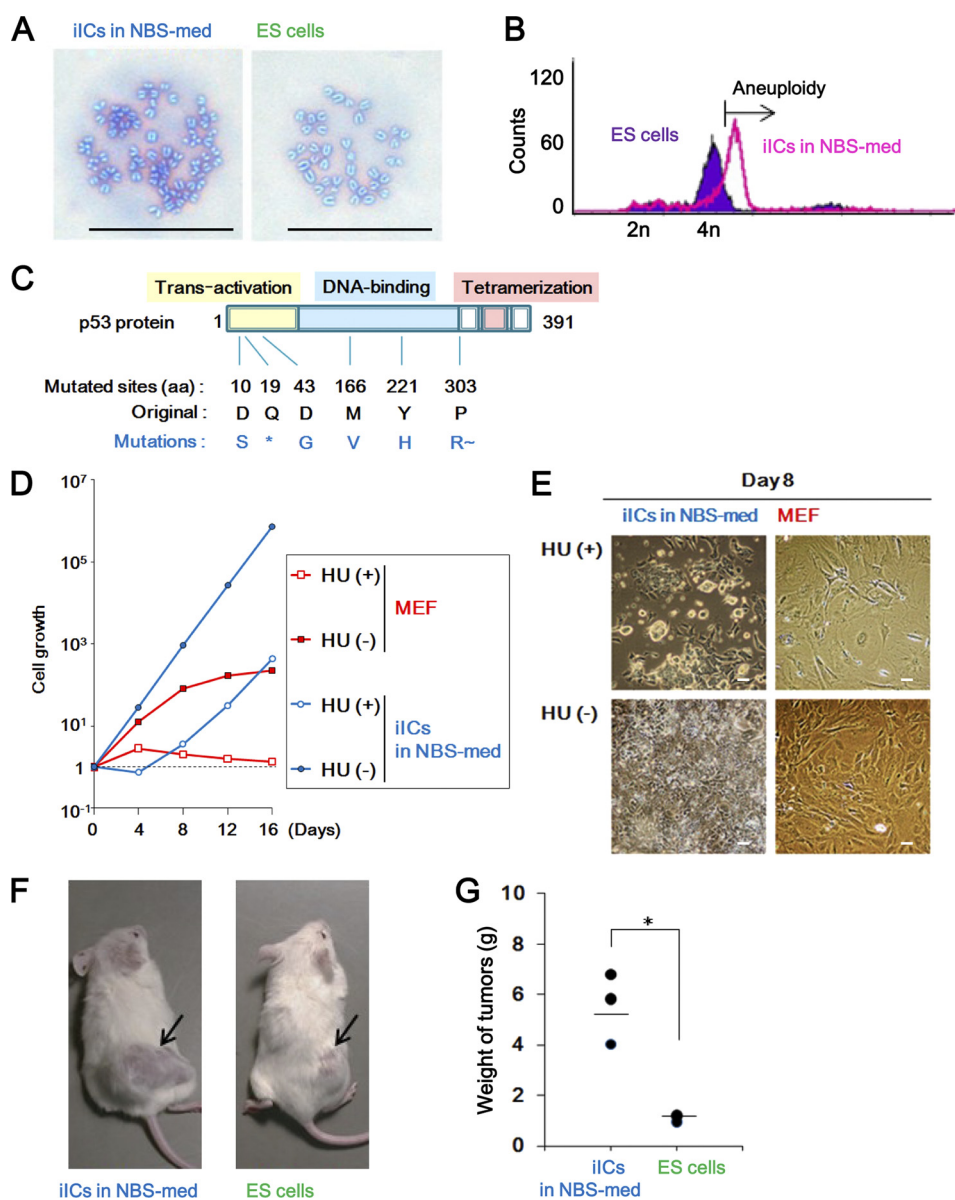
FIGURE 2. **iICs in NBS-med show cancerous characteristics.** *A* and *B*, aneuploidy is observed in iICs in NBS-med by Giemsa staining (*A*) and DNA content analysis (*B*) of M-phase cells. *C*, mutated p53 is frequently detected in iICs in NBS-med. The *asterisk* (*) indicates the stop codon. *R*~ indicates the resulting frameshift. *aa*, amino acids. *D* and *E*, the iICs in NBS-med show defective p53-dependent growth repression after treatment with low dose HU (0.2 mM). Growth curve (*D*) and morphology (*E*) are shown. *F* and *G*, enhanced tumorigenicity was observed in the iICs in NBS-med. *Arrows* indicate tumors (*F*) induced in NOD-SCID mice after transplantation. Tumor weights were measured 4 weeks after transplantation (*G*). *Scale bars*, 50 μm (*A* and *E*).

still maintained a largely undifferentiated status even under LIF withdrawal conditions. By contrast, the cGCs in FBS-med progressed through the steps of differentiation, lost *Klf4* expression, and acquired high expression of *Cdx2*, *Fgf5*, and *T* (Fig. 3*A*). Because *Klf4* expression is induced by LIF/Stat 3 signaling and implicated in ESC self-renewal (32), these results suggest that the acquisition of aberrant *Klf4* expression in iICs under NBS-med contributes to LIF-independent maintenance of an undifferentiated cell population. Furthermore, recent report showed that activated p53 promotes the differentiation of human ESCs by repressing the stem cell factors including Oct3/4 and Klf4 (33), implying that functional loss of p53-pathway also contributes the undifferentiated status in iICs in NBS-med.

FIGURE 1. **ESCs differentiating in NBS-med undergo senescence and subsequently aggregate in piled-up spheres.** *A*, an experimental design is shown. ESCs maintained with passaging every 2 days were held under three serum conditions. Cells were passaged as per ESC cultivation in each medium condition until passage 6 followed by continued maintenance with medium change. *B–D*, shown is piled-up sphere development via senescence. Representative images during differentiation induction in each condition are shown. After serial cell proliferation, cells in NBS-med senesced as indicated by the flattened and enlarged morphology (*B*; *arrows*) and β-galactosidase activity (*C*), which led to the development of piled-up colonies (representative image) (*D*). Cells in FBS-med did not show massive senescence (*B*; *arrows with dotted line*). ABS conditions did not induce subsequent proliferating cells (*B*, P6 + 14 days). *E* and *F*, piled-up sphere formation in each medium condition is shown. Although massive sphere development was observed in NBS-med, it was rarely observed in the other conditions. *G*, shown are normal MEFs senesced after serial proliferation, similar to the process seen during the differentiation of ESCs. *Scale bars*, 50 μm (*B–D* and *G*) or 2 cm (*E*).
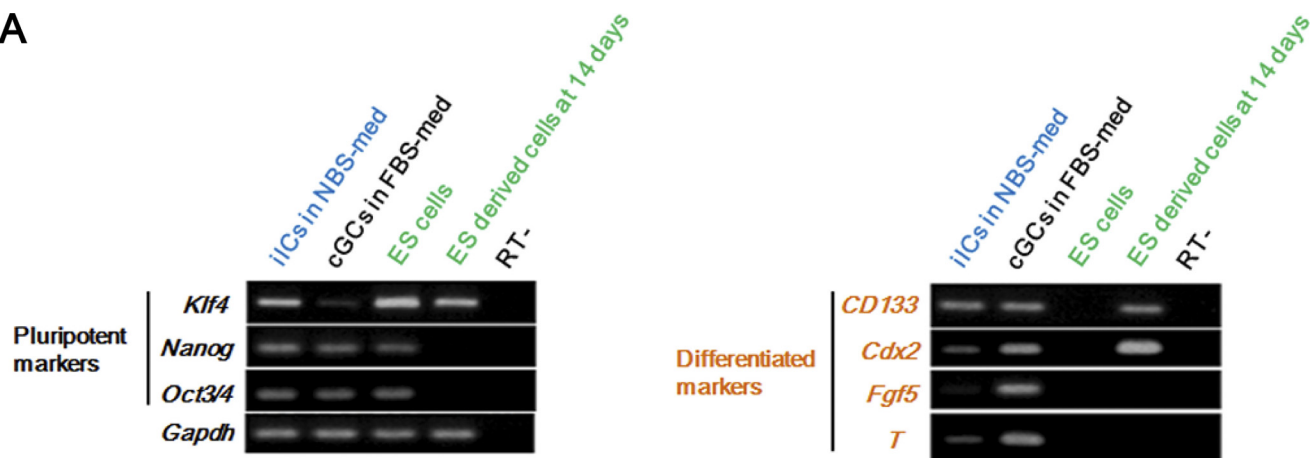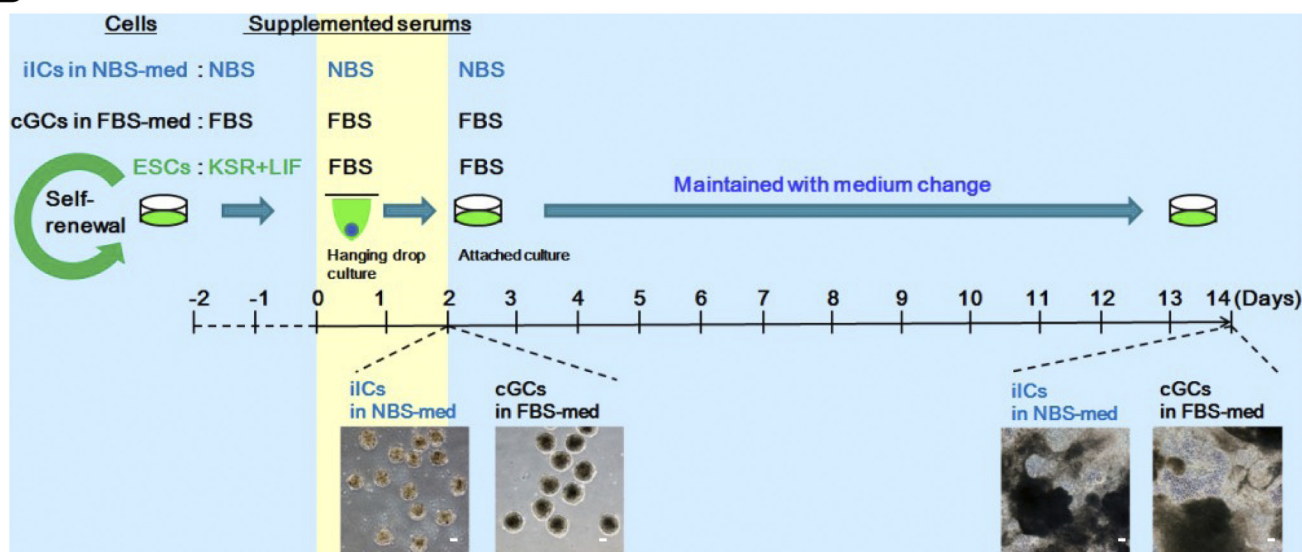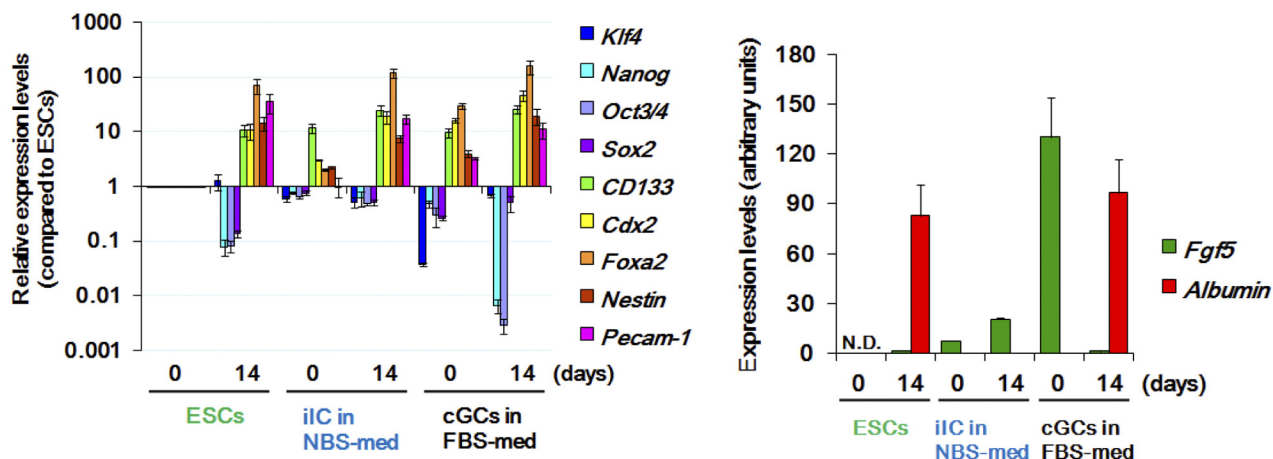
FIGURE 3. **iICs in NBS-med show stemness characteristics.** *A*, gene expression analysis is shown. Pluripotency and differentiation-associated gene expression status were compared in the indicated cells. ES derived cells at 14 days indicated the expression of each genes after differentiation for 14 days in a manner with Fig. 3*B*. *B*, experimental design is shown. Spontaneous differentiation was induced with EB formation by hanging-drop culture for 2 days and then seeded for attached culture. Inserted images are representative EBs (*left images*), and the resulting differentiated cells with multiple morphologies (*right images*) are indicated under each condition. *Scale bars*, 100 μm. *C*, gene expression analysis is shown. After differentiation induction, iICs in NBS-med still showed expression of pluripotency marker genes as well as differentiation marker genes in all germ layers.

To further investigate stem cell characteristics, we performed EB formation assays and examined self-renewal and differentiation capacities that are conserved in stem cells

including CSCs (Fig. 3*B*). During adherent culture of the induced EBs from iICs in NBS-med and cGCs in FBS-med, cells in each condition were migrated, massively prolifer-

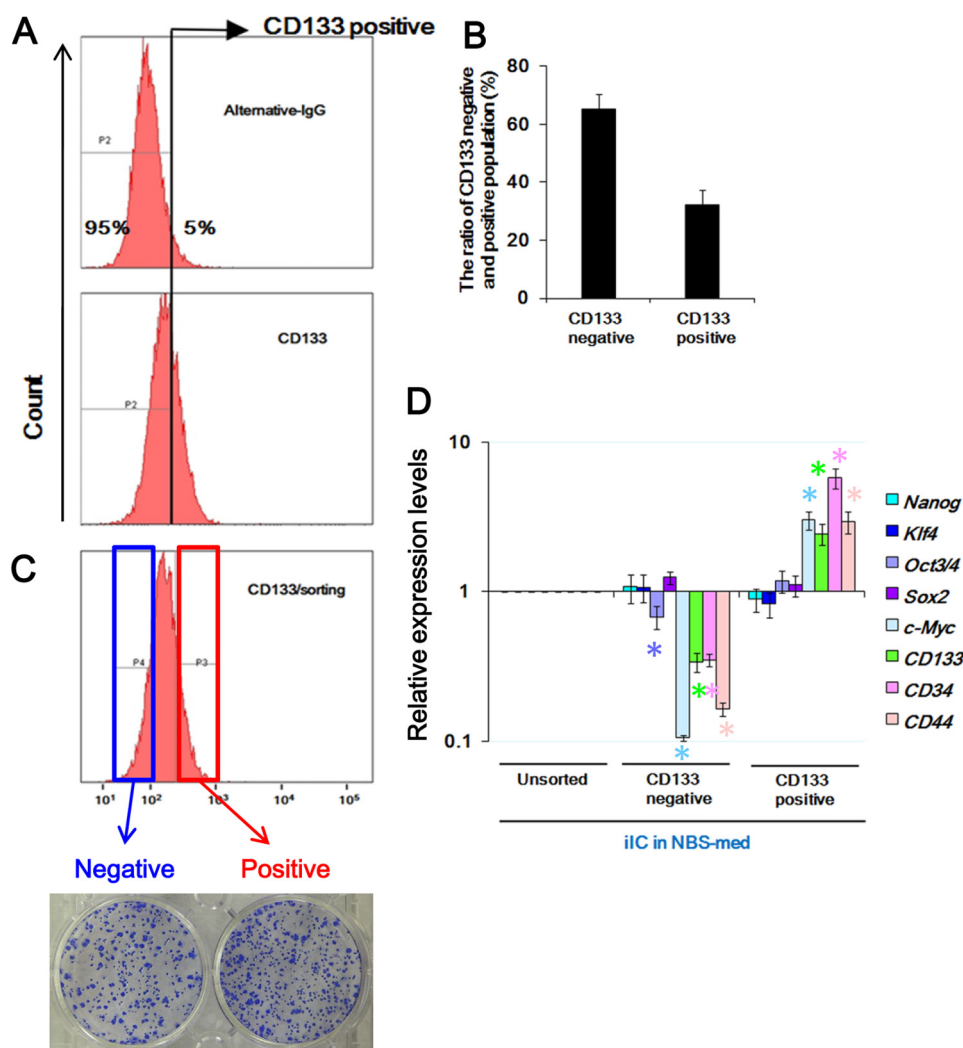FIGURE 4. **CSC markers are enriched in CD133-positive fractions of iICs in NBS-med.** *A* and *B*, FACS analysis identified CD133-positive cells in iICs in NBS-med. The threshold discriminating CD133 positive/negative fractions was determined by negative control experiments using alternative IgG (*A*, *upper*). The CD133 positive-fraction was about 35% of iICs in NBS-med (*A*, *lower*, and *B*). *C*, both CD133-positive and -negative fractions developed spheres on methylcellulose. *D*, expression of ES-related and CSC-related marker genes was compared between CD133-positive and -negative fractions. Expression of *Oct3/4*, *c-Myc*, and CSC-related marker genes is significantly high in CD133-positive fraction.

ated, and developed into cells with different morphologies (Fig. 3*B*, *inserted images*), implying differentiation of the iICs in NBS-med and cGCs in FBS-med. Consistently, after adherent culture for an additional 11 days after EB formation (see the *images* in Fig. 3*B*), the resulting EB cells in each condition showed expression of differentiation marker genes in all three germ layers (Fig. 3*C*). Such three germ layer differentiation was also shown in the tumors that developed with the experiments as in Fig. 2 and (supplemental Figs. S1 and S2). Tumor formation assay *in vivo* also confirmed the pluripotency of these cells (supplemental Fig. S2). Intriguingly, although the expression of pluripotency markers was largely decreased in cultured EB derived from the cGCs in FBS-med or ESCs, the iICs in NBS-med still showed high expression of pluripotent marker genes even after the induction of differentiation. This indicates that the iICs in NBS-med retain several stemness characteristics even under differentiation conditions, a feature that may confer an advantage in tumor formation. Indeed, pluripotent marker genes are still highly expressed in tumors derived from iICs

in NBS-med associated with enhanced tumor volume (supplemental Fig. S2 and Fig. 2). Taken together our results indicate that the iICs in NBS-med are effectively cancerous stem cells that show both cancer cell characteristics and stemness properties.

CSC-related Markers Accumulated in the CD133-enriched Fraction of iICs in NBS-med—CSCs are identified by several markers in surface antigens, such as CD133 (34). To characterize the stem-like subpopulation in the iICs in NBS-med, as shown in Fig. 4*A*, the CD133-positive fraction that is about 35% of iICs in NBS-med (Fig. 4*B*) was separated from the CD133-negative fraction. Although sphere formation efficiency on methylcellulose (Fig. 4*C*) and the expression of *Nanog*, *Klf4*, and *Sox2* were shown without a major difference in both CD133-positive and -negative fractions, *Oct3/4* and *c-Myc* expressions were significantly lower in the CD133-negative fraction (Fig. 4, *A* and *B*). In addition, other CSC markers *CD34* and *CD44* was also highly expressed in the CD133 enriched cells (Fig. 4*D*). These results imply that, as a stem-like subpopulation, CD133-positive fractions could contribute to the maintenance of iICs
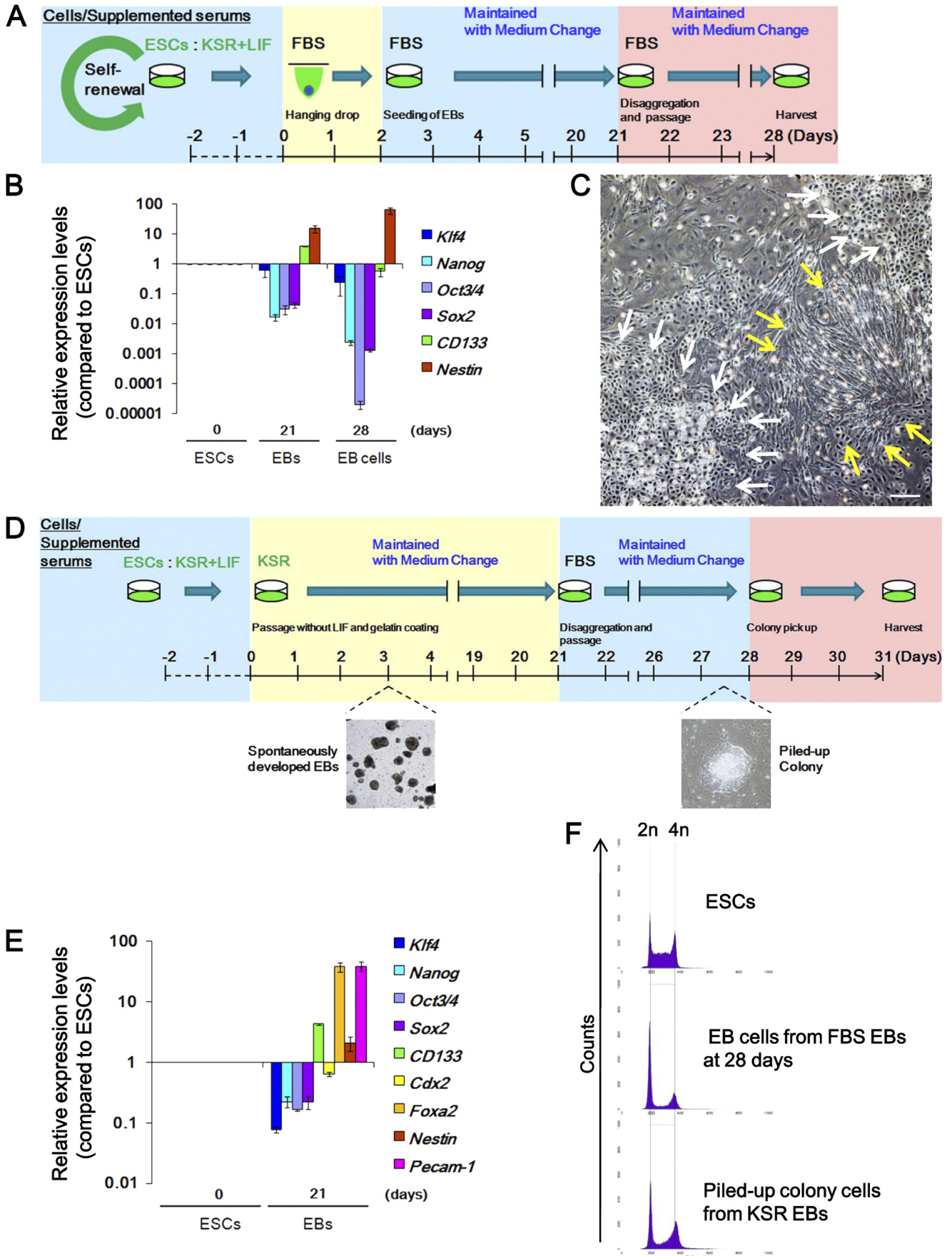
in NBS-med even under differentiation stress due to LIF independent expression of all Yamanaka factors (35). This identification poses another question in the status of cGCs in FBS-med.

cGCs in FBS-med Show Several Properties of Embryonal Carcinoma Cells—Similar to development of iICs under an aberrant serum environment, cGCs in FBS-med were also observed as a result of ESC cultivation under an aberrant serum environment compared with native development. As described above, the cGCs in FBS-med show neither the pile-up morphology nor major chromosomal instability and Arf-p53 module dysregulation (supplemental Fig. S1, *A* and *B*), suggesting that cGCs in FBS-med are not malignant cancerous cells. However, they still expressed some pluripotent marker genes and showed differentiation capacities to three germ layers with slightly enhanced tumorigenicity compared with ESCs (supplemental Fig. S1*D* and Fig. 3). Intriguingly, the characteristics of cGCs in FBS-med are shared with embryonal carcinoma cells that are developed from primordial germ cells derailing from the migration track as well as transplanted early stage embryos; embryonal carcinoma cells are characterized with tumorigenicity, the abilities of LIF-independent multipotency, and differentiation to three germ layers (2, 36), analogous to stemness characteristics shown in cGCs (supplemental Fig. S2 and Fig. 3). In addition, embryonal carcinoma cells are the pluripotent stem cells of teratocarcinoma with wild-type p53 and are quite responsive to chemotherapeutic drug treatment, which is also analogous to the features shown in cGCs (supplemental Fig. S2). Thus, a resulting population derived from the differentiated ESCs under an environmental aberrancy is analogous to that from the heterotopic transplantation of blastocysts and primordial germ cells.

Differentiation Environment in EBs Prevents Development of cGCs in FBS-med—Whereas ESCs as well as induced pluripotent stem cells possess the potential to enable regenerative medicine, this study poses the risk of development of CSCs and embryonal carcinoma cells under aberrant environments. This led us to investigate the CSC-like properties of ESC-derived cells that differentiated under several conditions *in vitro*. Expression of pluripotent marker genes were significantly reduced after differentiation by hanging drop culture in FBS-med at day 21 (Fig. 5, *A* and *B*). Such differentiated cells further underwent differentiation steps after disaggregating EBs and the additional adherent culture (Fig. 5*B*, *28 days*). Indeed, cells at 28 days massively differentiated in morphologically epithelial and fiber-like cells without detectable genomic instability (Fig. 5, *C* and *F*, *upper* and *middle*). Because non-serum conditions were also employed for ESC differentiation induction (37), genome stability was also tested under the conditions using KSR-med (Fig. 5*D*). ESCs in KSR/LIF($-$) medium spontaneously led to EB-like structure formation and underwent differ-

entiation (Fig. 5, *D* and *E*). Culture of dissolved EB cells led to some piled-up spheres in FBS-med (Fig. 5*D*); however, after cloning these spheres, most of them did not actively grow (22/24) (supplemental Fig. S3*A*) or show epithelial-like morphology (1/24) (supplemental Fig. S3*B*). Although a clone (1/24) could reform piled-up morphologies (supplemental Fig. S3*C*), the ability to form a piled-up sphere in such cells was much weaker than that of iICs in NBS-med (supplemental Fig. S3*C*) and did not accompany the chromosomal instability and Arf-p53 module dysregulation (Fig. 5*F*, *lower* and supplemental Fig. S3*D*). Together these results suggest the importance of *in vitro* differentiation conditions to reduce the risk of developing unexpected populations.

Differentiating ESCs Accumulate DNA Damage and Activate Anti-cancer Barrier Responses—Although this study illustrated that ESCs can transform into cancerous stem cells during differentiation in NBS-med, a question remains regarding the mechanistic aspects of the inductions of genomic instability, mutations, and the resulting transformation. Growth curves of differentiating ESCs in aberrant conditions demonstrate initial proliferation but then eventual cessation of growth in all three culture conditions (Fig. 6*A*). Under these processes, it was observed that some fraction of the cells naturally undergo apoptosis at around P2-P3, as assessed by TUNEL staining (Fig. 6*B* and supplemental Fig. S4*A*) and an increase of the sub-G_1 population by flow cytometry (Fig. 6*C* and supplemental Fig. S4*B*). γH2AX that appeared to reflect DNA damage started to be detected at P1 by Western blotting before apoptosis induction and by immunostained foci observed at P2 (Fig. 6*D*, *a* and *b*); however, the increased γH2AX level was efficiently decreased in P3 cells in FBS- and ABS-med, coincident with a decrease in apoptotic events (Fig. 6, *C* and *Db*, and supplemental Fig. S4, *C* and *D*). Together with the diminishment of H2AX in P3 cells (Fig. 6*Db*, compared with β-Actin signals) (38, 39), these results show that p53-dependent anti-cancer barrier reactions are activated in response to spontaneous DNA lesion formation, mirroring the initial stages of carcinogenesis.

ESCs Differentiating in NBS-med Undergo Senescence before the Development of Cancerous Stem Cells—Although carcinogenic stress and barrier responses were observed in differentiating ESCs under all three medium conditions, cancerous stem cells are only induced under NBS-med conditions. What exactly produces the difference in the differentiating ESCs? Unlike other conditions, damaged cells in NBS-med were not efficiently eliminated (Fig. 6*D*, *b* and *c*), thereby these cells with γH2AX but with diminished H2AX survived with a senescent morphology at P3-P5 (Fig. 1*B*, also see supplemental Fig. S4*D*), under which pile-up spheres were eventually developed. Together with the accelerated genomic instability under H2AX haploinsufficiency by exogenous DNA lesions (40), our observations imply that senescent

FIGURE 5. **Differentiation environments affect the reduction of risks for cancerous stem cell development.** *A*–*C*, differentiation of ESCs via EBs is shown. The experimental scheme is shown (*A*). EB dissociation and the following culture further led to differentiation in accordance with the decreased expression of ES-related and neural stem cell-related genes and enhanced expression of a premature neuron marker gene (*Nestin*) (*B*). At 28 days, ES-derived cells showed epithelial-like (*white arrows*) and fiber (*yellow arrows*) morphology. *D* and *E*, differentiation of ESCs in KSR-med is shown. The experimental scheme is shown (*D*). ESCs were also differentiated to three germ layers in KSR-med (*E*). Dissolved EBs were seeded in FBS-med condition or KSR condition, although dissolved EBs seeded into KSR-med massively died (data not shown). *F*, DNA content analysis in each state of cells is shown. Differentiating ESCs under FBS-med or KSR-med did not develop major genome instability. *Scale bars*, 50 μm.
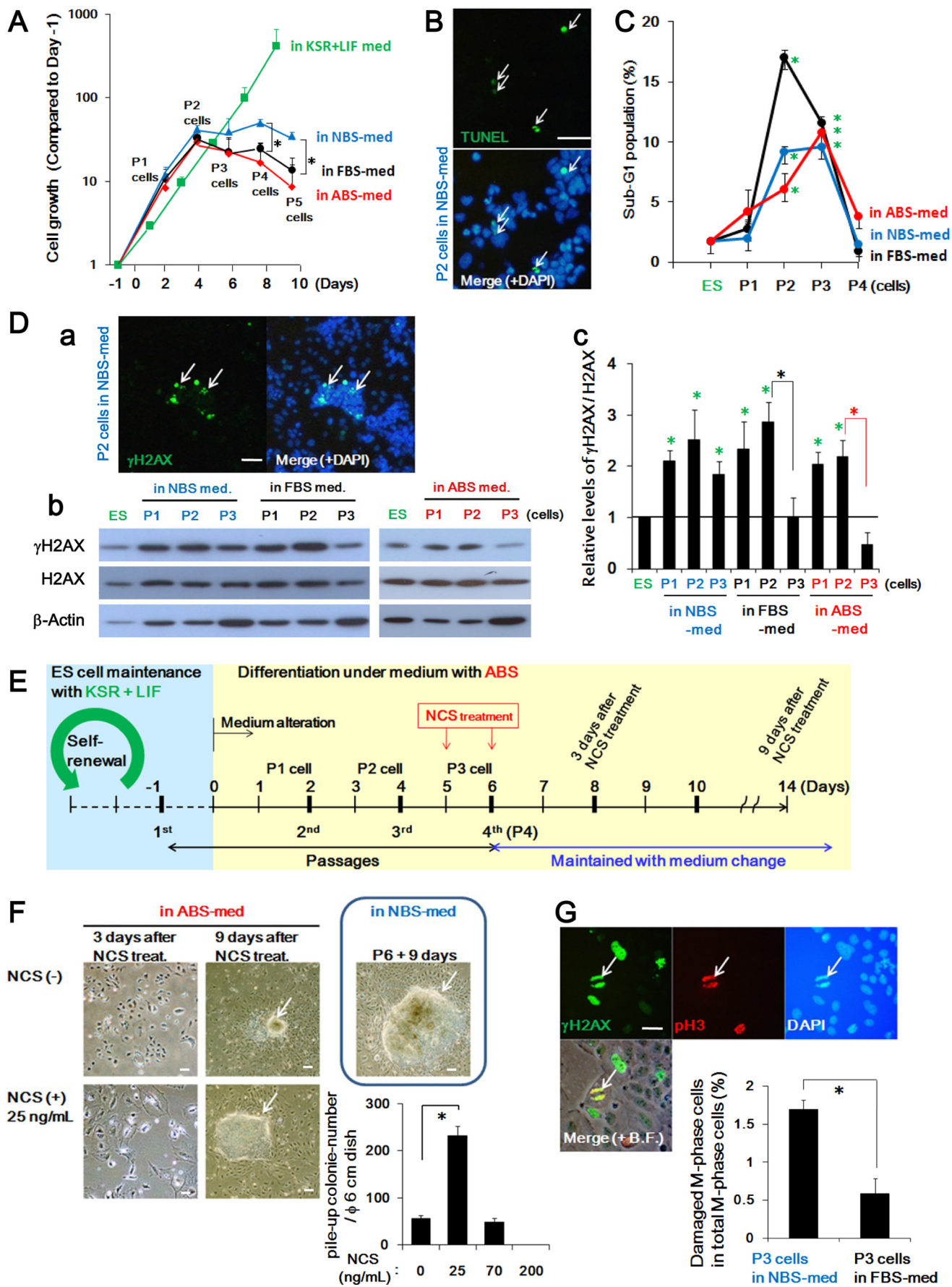
cells with irreparable DNA lesions undergo the carcinogenic transformation. To test this argument directly, we examined whether piled-up sphere formation was accelerated by the exogenous DNA lesions in the cells that have escaped the apoptotic event at P3. In ABS-med conditions, NCS treatment at 5 and 6 days promptly induced senescence-like morphology (Fig. 6, *E* and *F*, *3 days after NCS treatment*). At 9 days after NCS treatment, even in ABS-med conditions, NCS treatment induced piled-up sphere formation similar to the differentiating cells in NBS-med (Fig. 6*F*). Damage level was found to be critical to the frequency of pile-up sphere formation, which seemed to be optimum with 25 ng/ml NCS in this experiment (Fig. 6*F*). Thus, DNA lesions under down-regulated H2AX contribute to senescence induction in the differentiating ESCs and the resulting piled-up sphere formation.

Genomic instability development that is induced before MEF immortalization is ascribed to the carryover of irreparable DNA lesions to the M phase (8). In agreement with this, the irreparable DNA lesions in NBS-med were often carried over into the M phase of P3 cells before the development of iICs (Fig. 6*G*). Taken together, these results demonstrate that insufficient barrier reactions against carcinogenic stress permit the accumulation of aberrant DNA lesions in differentiating ESCs, leading into the development of induced cancerous stem cells.

A Condition with Lower FBS Concentration Leads to Accumulation of Senescent Cells under ESC Differentiation—The above results demonstrate that irreparable DNA lesions under diminished H2AX lead to senescence induction and resulting piled-up sphere formation during ESC differentiation. However, the question remains, Which factors in NBS-med conditions allow damaged cells to survive with senescence induction? To address this issue, we focused on the effect of growth acceleration that is produced by the different serum conditions and determined the effect of the exogenous growth acceleration by reducing the percentage of supplemented FBS (Fig. 7*A*) for the following reasons. 1) In the process of immortality development in MEFs, continuous growth acceleration by serum induces DNA double strand breaks due to DNA replication stress, which leads to the induction of senescence, genomic instability, and p53-module dysregulation, similar to the effect shown by oncogene acceleration (8, 38, 41, 42). 2) Temporary serum deprivation protects MEFs from immortality development under genome stability (38), suggesting that the level of growth acceleration could affect the balance between carcinogenic stress and an anti-cancer barrier. 3) During ESC differentiation we observed higher levels of subG$_1$ in FBS-med conditions compared with others (Fig. 6, *A* and *C*, *P2*), potentially suggesting that the difference in the enriched growth factors in FBS gives the difference in the stress-barrier balance. ESCs differentiated under 20, 10, and 5% FBS-med conditions initially proliferated in proportion to the serum concentration (Fig. 7*B*, *3 days*) and eventually stopped the growth (*6–9 days*). These differentiating cells exhibited γH2AX signaling (Fig. 7*C*, *3 and 6 days*) followed by H2AX diminishment (*9 days*). When γH2AX was presented, these cells were also subjected to apoptosis induction as shown by PARP1 cleavage (3 and 6 days) in all conditions, suggesting the activation of carcinogenic stress and the barrier responses. However, only in 10% FBS-med conditions, senescent cells are massively developed at 9 days, which was unexpectedly not shown either in higher or in lower serum conditions but only in the intermediate (Fig. 7*D*). These results illustrated that, for differentiating stem cells, a potential pitfall leading to senescence induction was generated between growth stimulation levels in the surrounding environment, probably associated with the balance between the barrier responses and cell maintenance.
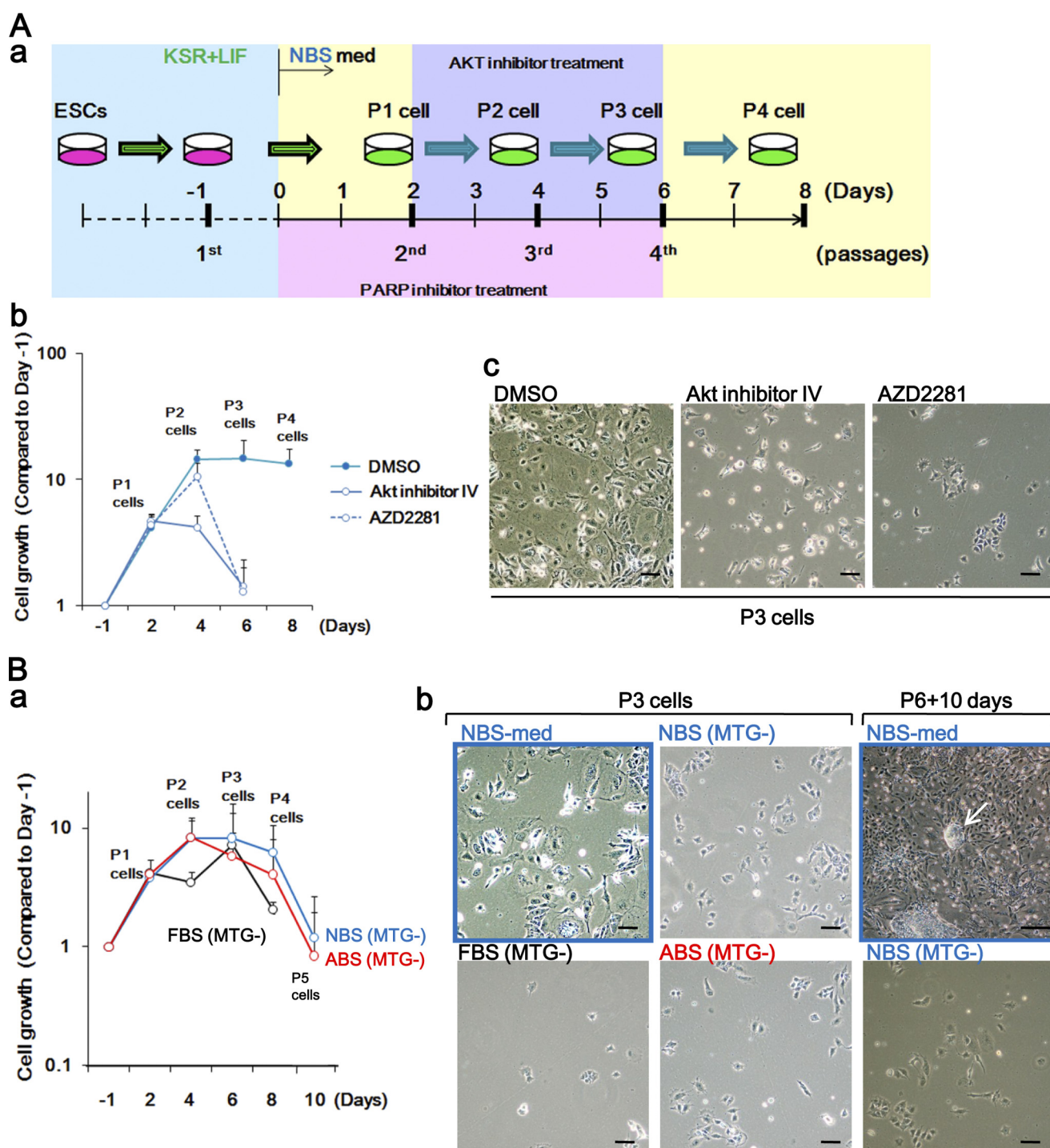
Sufficient Barrier Reactions Prevent Senescence Induction in Differentiating ESCs—To prevent cancer stem cell development, the above results suggest that sufficient barrier activation protects the damaged cells from senescence and the resulting transformation. To confirm this issue, we treated P1 and P2 cells in NBS-med with Akt inhibitor IV and PARP inhibitor AZD2281 (Fig. 8*Aa*) because Akt is a major target of several anti-cancer drugs, such as sorafenib (43, 44) and PARP inhibitors also act as an anti-cancer drug (45). As expected, treatment of Akt inhibitor IV or AZD2281 significantly reduced the surviving cells during differentiation of ESCs in NBS-med (Fig. 8*Ab* and supplemental Fig. S5), associating with the protection from the accumulation of senescent cells (Fig. 8*Ac*). Because an effect of PARP inhibition is partial DNA repair deficiency, the effect of spontaneous DNA damage was further tested by withdrawal of monothioglycerol that reduces reactive oxygen species that lead to stress and contributes to the reduction of DNA damage (46–48). Again, culture conditions without monothioglycerol led neither to survival with a senescent state nor to the development of piled-up spheres (Fig. 8*B*). This supports that sufficient barrier activation prevents cancerous stem cell development, in which appropriate treatment with an anti-cancer drug might help. However, such an argument might be carefully treated because the effects of DNA damage could lead to different outputs which depend on cellular conditions (Fig. 6, *E* and *F*).

FIGURE 6. **Carcinogenic stress is induced during differentiation of ESCs in aberrant environments.** *A*, cell growth in each medium condition is shown. Unlike continuously growing ESCs in the KSR + LIF condition, differentiating cells under each condition were growth-arrested at P2-P3. *B* and *C*, massive apoptosis induction was observed at P2-P3 with the TUNEL assay (*B*) and sub-G$_1$ fractions (*C*). *ES*, embryonic stem. Sub-G$_1$ fraction analysis revealed that apoptosis is mainly induced at P2-P3, which coincides with growth suppression (*A*). *D*, the status of spontaneously accumulated DNA lesions was determined by γH2AX foci formation (*Da*, also demonstrated in supplemental Fig. S3C) as well as γH2AX signal detection with Western blotting (*Db*). γH2AX signals were diminished at P3 in the differentiating cells in FBS- and ABS-med but not significantly decreased in cells in NBS-med (see *P2* and *P3* and quantified Fig. 4*Dc*). *E* and *F*, additional DNA damage accelerates the piled-up sphere formation. Experimental design is shown in *E*. ESCs were maintained and differentiated in ABS-med as in Fig. 1*A*, but the P3 cells in P3 + 1 day were treated with NCS for 3 days. After NCS treatment, cells were maintained with medium change as cells rapidly senesced (*F*, *3 days after NCS treatment*). NCS treatment allows differentiating ESCs to form spheres in ABS-med. Images are representative, showing senescent cells, and resulting sphere development was induced under ABS-med with 25 ng/ml NCS treatment (*F*). The frequency of piled-up sphere development in ABS-med was also determined with different NCS doses (*F*, *graph*). Different than the Fig. 1 results, we observed piled-up colony formation in non-NCS-treated conditions, implying that a decrease in the times of passage allowed remaining undifferentiated cell proliferation. *Scale bars*, 100 μm. *G*, the status of DNA lesions in M-phase cells was determined by co-localized staining of γH2AX and phosphorylated histone H3 (pH3) (*arrows*). Images are representative. The quantified results are also shown (*graph*), indicating DNA-lesion carryover into the M phase. *Scale bars*, 50 μm.
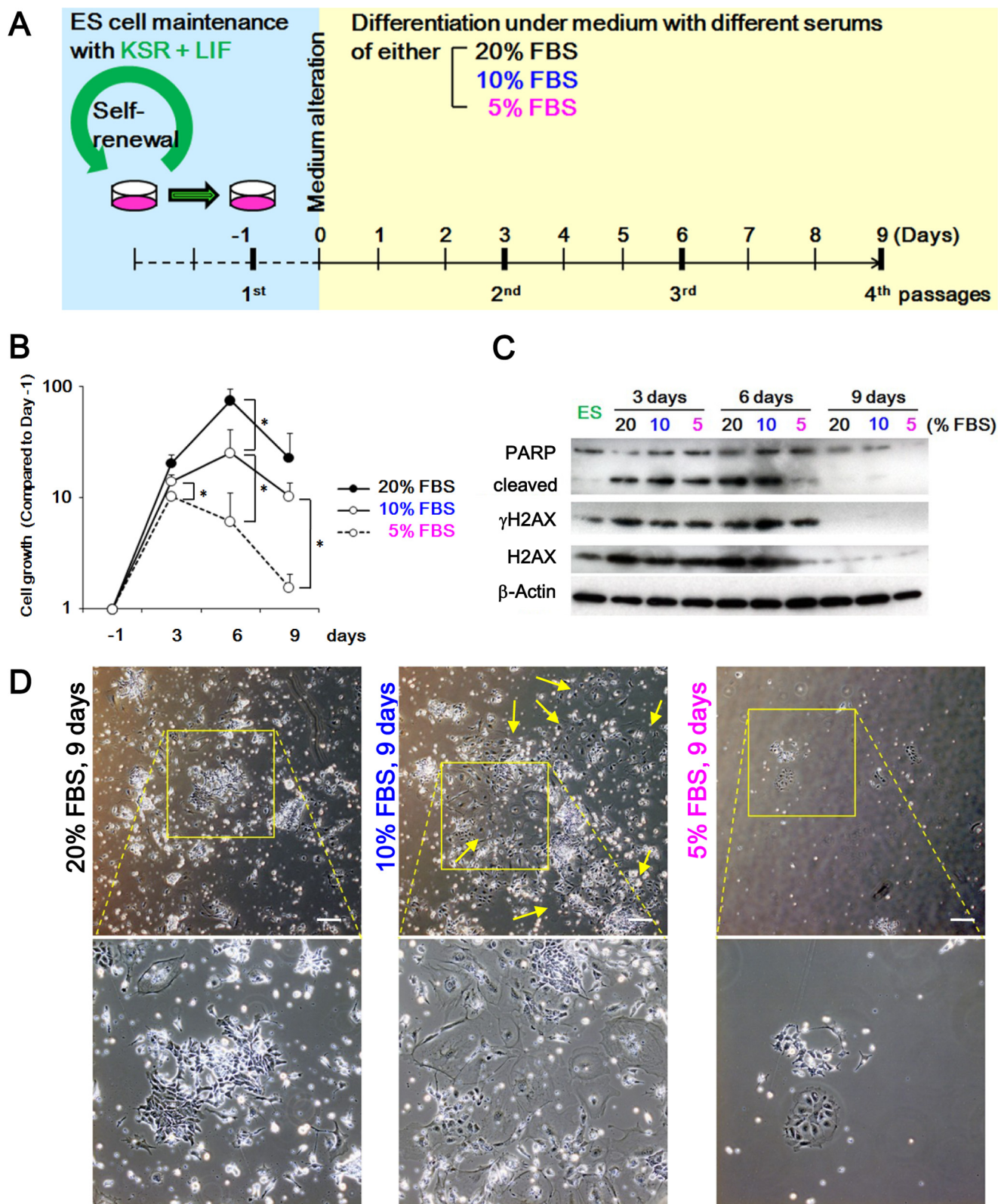
FIGURE 7. **Decreased intensity of growth acceleration could induce senescence-like morphology of differentiating ESCs in FBS-med.** *A*, experimental design is shown. ESCs maintained with passaging every 2 days were held under 20, 10. Cells were passaged every 3 days in each medium condition until 9 days. *B*, shown is the growth curve of differentiating ESCs in the indicated conditions. A high concentration of FBS induced strong cell proliferation. *C*, DNA damage response in differentiating ESCs is shown. Western blotting shows PARP1 cleavage (3 and 6 days), γH2AX up-regulation (3 and 6 days), and H2AX diminishment (9 days) in differentiating ESCs. ES, *ES*, embryonic stem. *D*, cell morphologies in each medium at 9 days is shown. Senescence was not observed in 20 and 5% FBS condition, but differentiating ESCs in 10% FBS condition showed flattened and enlarged morphology. *Lower panels* show expanded images of the squares in the *upper panels*. *Yellow arrows* indicate the representative cells showing flattened and enlarged morphology. *Scale bars*, 50 μm.

FIGURE 8. **Sufficient barrier response protects differentiating ESCs from senescence, preventing the development of cancerous stem cells.** *A*, protection of differentiating ESCs from senescence by treatment with anti-cancer drugs is shown. The experimental scheme is shown (*a*). Akt inhibitor IV and PARP inhibitor AZD2281 led to the reduction of surviving cells (*b*) and senescent cells (*c*). *B*, prevention of cancerous stem cell development in the presence of ROS is shown. Development of cancerous stem cells under NBS-med was inhibited in the absence of monothioglycerol (*MTG*) as shown in the lower cell survival (a, compared with Fig. 6A), inhibition of senescence (*b*, *P3 cells*), and no piled-up sphere development (*b*, *P6 + 10 days*). The *arrow* indicates the sphere development in control conditions. *Scale bars*, 50 μm.

DISCUSSION

Our results illustrated that ESCs differentiating under aberrant conditions, such as cultivation in NBS-med, are subject to carcinogenic stress, resulting in genomic instability, mutation in the *p53* locus, and the appearance of cancerous stem cells (Fig. 9). Although senescing MEFs subjected to carcinogenic stress develop immortality without accompanying stemness and tumorigenicity (10), similar stresses in differentiating ESCs are associated with the development of malignancy. Thus, unlike differentiated cells, ESCs differentiating under environmental aberrancy suffer potentially from a risk of developing into cancerous stem cells upon spontaneous exposure to carcinogenic stress.
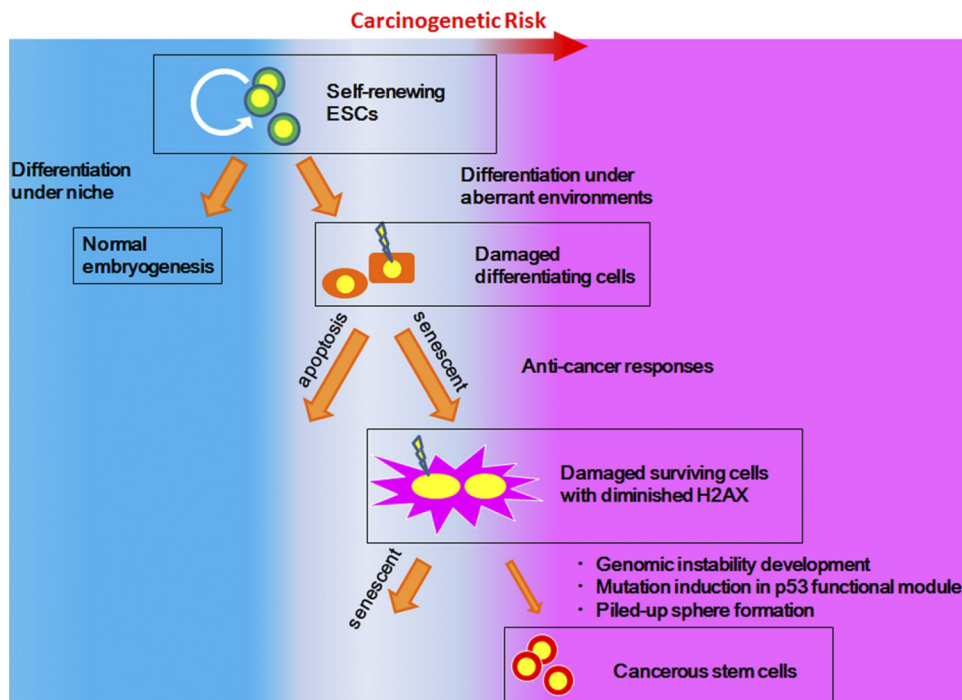
FIGURE 9. **Model.** In the process of ESC differentiation, cells subjected to environmental aberrancies are subjected to carcinogenic stress, resulting in the emergence of cancerous stem cells with genomic instability and mutations in p53 or Arf-p53 pathways.

Before their development into cancerous stem cells, ESCs differentiating in aberrant serum environments emulate cells in the initial stages of carcinogenesis, during which time they accumulate DNA lesions and exhibit barrier reactions, such as the induction of senescence and apoptosis. Genomic instability and mutations are also induced during the initial stages, contributing not only to the development of immortality but also to the acquisition of aberrant stemness characteristics that include the retention of stemness marker gene expression even under differentiation conditions. Thus, cancerous stem cells can propagate without losing stemness properties even in environments in which normal stem cells cannot maintain their undifferentiated status.

The development of CSCs is critical for carcinogenesis. In a manner analogous to the transformation of ESCs into cancerous stem cells, differentiating somatic stem cells can also be transformed into CSCs *in vivo* due to aberrant niche environments. This is supported by several documented observations: 1) age is a risk factor for defective niche function (23), 2) hematopoietic stem cells spontaneously accumulate endogenous DNA damage with age (49), and 3) disruption of the hematopoietic niche induces differentiation disorders in progenitor cells and secondary oncogenesis (22). In addition, humoral factors could be involved in the balance between progression and prevention of carcinogenic transformation; differentiating ESCs under NBS-med override the anti-cancer barrier and result in the development of cancerous stem cells, whereas those under FBS- and ABS-med are blocked. Importantly, this indicates that some conditions effectively induce anti-cancer barriers, as observed in FBS- and ABS-med, although this balance can also be altered by exogenous DNA damage. Thus, our results illustrate that normal stem cells can transform into CSCs during differentiation in aberrant environments and sug-

gest that the development of CSCs is prevented by effective induction of anti-cancer barrier responses, pointing to a potential target for cancer prevention.

REFERENCES

1. Wicha, M. S., Liu, S., and Dontu, G. (2006) Cancer stem cells. An old idea, a paradigm shift. *Cancer Res.* **66,** 1883–1890
2. Werbowetski-Ogilvie, T. E., and Bhatia, M. (2008) Pluripotent human stem cell lines. What we can learn about cancer initiation. *Trends Mol. Med.* **14,** 323–332
3. Chiba, T., Zheng, Y. W., Kita, K., Yokosuka, O., Saisho, H., Onodera, M., Miyoshi, H., Nakano, M., Zen, Y., Nakanuma, Y., Nakauchi, H., Iwama, A., and Taniguchi, H. (2007) Enhanced self-renewal capability in hepatic stem/progenitor cells drives cancer initiation. *Gastroenterology* **133,** 937–950
4. Liu, Y., Clem, B., Zuba-Surma, E. K., El-Naggar, S., Telang, S., Jenson, A. B., Wang, Y., Shao, H., Ratajczak, M. Z., Chesney, J., and Dean, D. C. (2009) Mouse fibroblasts lacking RB1 function form spheres and undergo reprogramming to a cancer stem cell phenotype. *Cell Stem Cell* **4,** 336–347
5. Bartkova, J., Horejsí, Z., Koed, K., Krämer, A., Tort, F., Zieger, K., Guldberg, P., Sehested, M., Nesland, J. M., Lukas, C., Ørntoft, T., Lukas, J., and Bartek, J. (2005) DNA damage response as a candidate anti-cancer barrier in early human tumorigenesis. *Nature* **434,** 864–870
6. Gorgoulis, V. G., Vassiliou, L. V., Karakaidos, P., Zacharatos, P., Kotsinas, A., Liloglou, T., Venere, M., Ditullio, R. A., Jr., Kastrinakis, N. G., Levy, B., Kletsas, D., Yoneta, A., Herlyn, M., Kittas, C., and Halazonetis, T. D. (2005) Activation of the DNA damage checkpoint and genomic instability in human precancerous lesions. *Nature* **434,** 907–913
7. Bartkova, J., Rezaei, N., Liontos, M., Karakaidos, P., Kletsas, D., Issaeva, N., Vassiliou, L. V., Kolettas, E., Niforou, K., Zoumpourlis, V. C., Takaoka, M., Nakagawa, H., Tort, F., Fugger, K., Johansson, F., Sehested, M., Andersen, C. L., Dyrskjot, L., Ørntoft, T., Lukas, J., Kittas, C., Helleday, T., Halazonetis, T. D., Bartek, J., and Gorgoulis, V. G. (2006) Oncogene-induced senescence is part of the tumorigenesis barrier imposed by DNA damage checkpoints. *Nature* **444,** 633–637
8. Ichijima, Y., Yoshioka, K., Yoshioka, Y., Shinohe, K., Fujimori, H., Unno, J., Takagi, M., Goto, H., Inagaki, M., Mizutani, S., and Teraoka, H. (2010) DNA lesions induced by replication stress trigger mitotic aberration and

tetraploidy development. *PLoS One* **5,** e8821

9. Matheu, A., Maraver, A., Klatt, P., Flores, I., Garcia-Cao, I., Borras, C., Flores, J. M., Viña, J., Blasco, M. A., and Serrano, M. (2007) Delayed ageing through damage protection by the *Arf/p53* pathway. *Nature* **448,** 375–379

10. Sun, H., and Taneja, R. (2007) Analysis of transformation and tumorigenicity using mouse embryonic fibroblast cells. *Methods Mol. Biol.* **383,** 303–310

11. Yang, Y. M., and Chang, J. W. (2008) Current status and issues in cancer stem cell study. *Cancer Invest.* **26,** 741–755

12. Kim, J. H., Kim, S. H., Hahn, E. W., and Song, C. W. (1978) 5-Thio-D-glucose selectively potentiates hyperthermic killing of hypoxic tumor cells. *Science* **200,** 206–207

13. Bunting, K. D. (2002) ABC transporters as phenotypic markers and functional regulators of stem cells. *Stem Cells* **20,** 11–20

14. Seaberg, R. M., and van der Kooy, D. (2003) Stem and progenitor cells. The premature desertion of rigorous definitions. *Trends Neurosci.* **26,** 125–131

15. Leahy, A., Xiong, J. W., Kuhnert, F., and Stuhlmann, H. (1999) Use of developmental marker genes to define temporal and spatial patterns of differentiation during embryoid body formation. *J. Exp. Zool.* **284,** 67–81

16. Kondoh, H., Lleonart, M. E., Gil, J., Wang, J., Degan, P., Peters, G., Martinez, D., Carnero, A., and Beach, D. (2005) Glycolytic enzymes can modulate cellular life span. *Cancer Res.* **65,** 177–185

17. Dontu, G., El-Ashry, D., and Wicha, M. S. (2004) Breast cancer, stem/progenitor cells, and the estrogen receptor. *Trends Endocrinol. Metab.* **15,** 193–197

18. Jones, D. L., and Wagers, A. J. (2008) No place like home. Anatomy and function of the stem cell niche. *Nat. Rev. Mol. Cell Biol.* **9,** 11–21

19. Knoepfler, P. S. (2009) Deconstructing stem cell tumorigenicity. A roadmap to safe regenerative medicine. *Stem Cells* **27,** 1050–1056

20. Morange, M. (2006) What history tells us VII. Twenty-five years ago. The production of mouse embryonic stem cells. *J. Biosci.* **31,** 537–541

21. Wylie, C. (1999) Germ cells. *Cell* **96,** 165–174

22. Raaijmakers, M. H., Mukherjee, S., Guo, S., Zhang, S., Kobayashi, T., Schoonmaker, J. A., Ebert, B. L., Al-Shahrour, F., Hasserjian, R. P., Scadden, E. O., Aung, Z., Matza, M., Merkenschlager, M., Lin, C., Rommens, J. M., and Scadden, D. T. (2010) Bone progenitor dysfunction induces myelodysplasia and secondary leukemia. *Nature* **464,** 852–857

23. Smith, J. A., and Daniel, R. (2012) Stem cells and aging: a chicken-or-the-egg issue? *Aging Dis.* **3,** 260–268

24. Fujimori, H., Asahina, K., Shimizu-Saito, K., Ikeda, R., Tanaka, Y., Teramoto, K., Morita, I., and Teraoka, H. (2008) Vascular endothelial growth factor promotes proliferation and function of hepatocyte-like cells in embryoid bodies formed from mouse embryonic stem cells. *J. Hepatol.* **48,** 962–973

25. Marusyk, A., Wheeler, L. J., Mathews, C. K., and DeGregori, J. (2007) p53 mediates senescence-like arrest induced by chronic replication stress. *Mol. Cell. Biol.* **27,** 5336–5351

26. Fernandes, K. J., McKenzie, I. A., Mill, P., Smith, K. M., Akhavan, M., Barnabé-Heider, F., Biernaskie, J., Junek, A., Kobayashi, N. R., Toma, J. G., Kaplan, D. R., Labosky, P. A., Rafuse, V., Hui, C. C., and Miller, F. D. (2004) A dermal niche for multipotent adult skin-derived precursor cells. *Nat. Cell Biol.* **6,** 1082–1093

27. Lee, B. Y., Han, J. A., Im, J. S., Morrone, A., Johung, K., Goodwin, E. C., Kleijer, W. J., DiMaio, D., and Hwang, E. S. (2006) Senescence-associated β-galactosidase is lysosomal β-galactosidase. *Aging Cell* **5,** 187–195

28. Masaki, H., Nishida, T., Kitajima, S., Asahina, K., and Teraoka, H. (2007) Developmental pluripotency-associated 4 (DPPA4) localized in active chromatin inhibits mouse embryonic stem cell differentiation into a primitive ectoderm lineage. *J. Biol. Chem.* **282,** 33034–33042

29. Nitou, M., Sugiyama, Y., Ishikawa, K., and Shiojiri, N. (2002) Purification of fetal mouse hepatoblasts by magnetic beads coated with monoclonal anti-e-cadherin antibodies and their *in vitro* culture. *Exp. Cell Res.* **279,** 330–343

30. Lengauer, C., Kinzler, K. W., and Vogelstein, B. (1998) Genetic instabilities in human cancers. *Nature* **396,** 643–649

31. Sherr, C. J., and McCormick, F. (2002) The RB and p53 pathways in cancer. *Cancer Cell* **2,** 103–112

32. Zhang, P., Andrianakos, R., Yang, Y., Liu, C., and Lu, W. (2010) Kruppel-like factor 4 (Klf4) prevents embryonic stem (ES) cell differentiation by regulating Nanog gene expression. *J. Biol. Chem.* **285,** 9180–9189

33. Jain, A. K., Allton, K., Iacovino, M., Mahen, E., Milczarek, R. J., Zwaka, T. P., Kyba, M., and Barton, M. C. (2012) p53 regulates cell cycle and microRNAs to promote differentiation of human embryonic stem cells. *PLoS Biol.* **10,** e1001268

34. Ferrandina, G., Petrillo, M., Bonanno, G., and Scambia, G. (2009) Targeting CD133 antigen in cancer. *Expert Opin. Ther. Targets* **13,** 823–837

35. Takahashi, K., and Yamanaka, S. (2006) Induction of pluripotent stem cells from mouse embryonic and adult fibroblast cultures by defined factors. *Cell* **126,** 663–676

36. Spierings, D. C., de Vries, E. G., Vellenga, E., and de Jong, S. (2003) The attractive Achilles heel of germ cell tumors. An inherent sensitivity to apoptosis-inducing stimuli. *J. Pathol.* **200,** 137–148

37. Oh, S. K., and Choo, A. B. (2006) Human embryonic stem cells. Technological challenges toward therapy. *Clin. Exp. Pharmacol. Physiol.* **33,** 489–495

38. Atsumi, Y., Fujimori, H., Fukuda, H., Inase, A., Shinohe, K., Yoshioka, Y., Shikanai, M., Ichijima, Y., Unno, J., Mizutani, S., Tsuchiya, N., Hippo, Y., Nakagama, H., Masutani, M., Teraoka, H., and Yoshioka, K. (2011) Onset of quiescence following p53-mediated down-regulation of H2AX in normal cells. *PLoS One* **6,** e23432

39. Yoshioka, K., Atsumi, Y., Fukuda, H., Masutani, M., and Teraoka, H. (2012) The quiescent cellular state is *Arf/p53*-dependent and associated with H2AX down-regulation and genome stability. *Int. J. Mol. Sci.* **13,** 6492–6506

40. Celeste, A., Difilippantonio, S., Difilippantonio, M. J., Fernandez-Capetillo, O., Pilch, D. R., Sedelnikova, O. A., Eckhaus, M., Ried, T., Bonner, W. M., and Nussenzweig, A. (2003) H2AX haploinsufficiency modifies genomic stability and tumor susceptibility. *Cell* **114,** 371–383

41. Woo, R. A., and Poon, R. Y. (2004) Activated oncogenes promote and cooperate with chromosomal instability for neoplastic transformation. *Genes Dev.* **18,** 1317–1330

42. Deckbar, D., Birraux, J., Krempler, A., Tchouandong, L., Beucher, A., Walker, S., Stiff, T., Jeggo, P., and Löbrich, M. (2007) Chromosome breakage after G_2 checkpoint release. *J. Cell Biol.* **176,** 749–755

43. Oh, S. J., Erb, H. H., Hobisch, A., Santer, F. R., and Culig, Z. (2012) Sorafenib decreases proliferation and induces apoptosis of prostate cancer cells by inhibition of the androgen receptor and Akt signaling pathways. *Endocr. Relat. Cancer* **19,** 305–319

44. Mitsiades, C. S., Mitsiades, N., and Koutsilieris, M. (2004) The Akt pathway. Molecular targets for anti-cancer drug development. *Curr. Cancer Drug Targets* **4,** 235–256

45. Fong, P. C., Boss, D. S., Yap, T. A., Tutt, A., Wu, P., Mergui-Roelvink, M., Mortimer, P., Swaisland, H., Lau, A., O'Connor, M. J., Ashworth, A., Carmichael, J., Kaye, S. B., Schellens, J. H., and de Bono, J. S. (2009) Inhibition of poly(ADP-ribose) polymerase in tumors from BRCA mutation carriers. *N. Engl. J. Med.* **361,** 123–134

46. Parrinello, S., Samper, E., Krtolica, A., Goldstein, J., Melov, S., and Campisi, J. (2003) Oxygen sensitivity severely limits the replicative lifespan of murine fibroblasts. *Nat. Cell Biol.* **5,** 741–747

47. Wiles, M. V., and Keller, G. (1991) Multiple hematopoietic lineages develop from embryonic stem (ES) cells in culture. *Development* **111,** 259–267

48. Guachalla, L. M., and Rudolph, K. L. (2010) ROS induced DNA damage and checkpoint responses. Influences on aging? *Cell Cycle* **9,** 4058–4060

49. Rossi, D. J., Bryder, D., Seita, J., Nussenzweig, A., Hoeijmakers, J., and Weissman, I. L. (2007) Deficiencies in DNA damage repair limit the function of hematopoietic stem cells with age. *Nature* **447,** 725–729